Available online at www.sciencedirect.com
ScienceDirect
Journal of Sound and Vibration 310 (2008) 812–828
JOURNAL OF SOUND AND VIBRATION
www.elsevier.com/locate/jsvi

Contributions of standing-wave components to dynamic stresses in a beam

X.Q. Wang*, R.M.C. So, K.T. Chan

Department of Mechanical Engineering, The Hong Kong Polytechnic University, Hung Hom, Kowloon, Hong Kong SAR, PR China

Received 14 June 2006; received in revised form 6 June 2007; accepted 7 June 2007
Available online 21 December 2007

Abstract

Vibration modes of a beam have been identified previously as superposed standing waves, each of which consisting of two components, denoted by k_a and k_b, respectively. In this paper, individual contributions of these two components to dynamic normal and shear stresses in a beam are investigated, and their roles in the development of cracks in a beam are briefly addressed. A cantilever beam subject to an impulse tip force of different time durations is chosen as an example to illustrate their respective effects. The contributions of the k_b-component are studied in particular, since it changes its wave characteristics from evanescent to propagating when its frequency exceeds the critical frequency. For an impulse force of long duration, it is shown that the k_b-component is dominant in the normal stress while the k_a-component is dominant in the shear stress. They would play dominant roles for Mode I and Mode II of crack propagation, respectively. For an impulse force of short duration, both normal and shear stresses are dominated by the k_a-component. Therefore, the k_a-component would play a dominant role for both Mode I and Mode II of crack propagation. It should be noted, however, k_a- and k_b-components above the critical frequency contribute almost equally to both normal and shear stresses, regardless of the duration of the force.

1. Introduction

Dynamic response of beam-type structural and machinery components subjected to time-variant loadings is an important issue to be considered in engineering design if failure due to fatigue is to be avoided. It is well known that there exists a yield stress for a structure, beyond which the structure will experience irreversible plastic deformation. In the case of dynamic loading, however, failure might occur at a level of stress much less than the yield stress. The stress-cycle diagram is usually used to determine an endurance limit for a safe strength. For such a purpose, an analysis of dynamic stresses is necessary.

In this paper, an analysis of the contributions of different standing-wave components to dynamic stresses in a beam is presented. While steady-state response of a beam subjected to external excitation has been investigated extensively (e.g., Ref. [1]), the study of dynamic stresses in a beam is scarce. Roy and Ganesan [2]

*Corresponding author. Tel.: +852 27664502; fax: +852 23654703.
E-mail address: mmxqwang@polyu.edu.hk (X.Q. Wang).

0022-460X/$ - see front matter © 2007 Elsevier Ltd. All rights reserved.
doi:10.1016/j.jsv.2007.06.006

considered a cantilever beam subjected to an impulse loading at the tip, showing that the contribution of higher modes in the dynamic stress becomes important for an impulse loading of short duration.

In the study of Roy and Ganesan [2], the Euler–Bernoulli beam theory was used to model the beam where the effects of shear deformation and rotary inertia were neglected. While this model gives good prediction in the low-frequency range, it may not be sufficient for a beam subjected to impulse loading since the response covers the whole frequency spectrum. The physics of beam vibration at high frequencies is not correctly described by using this model [3]. When a beam is vibrating, its motion is represented by both transverse displacement and bending rotation. They are not directly related as suggested by the Euler–Bernoulli theory, but coupled through shear deformation as described by the Timoshenko beam theory. Chan et al. [4] showed that, in general, the vibration mode of a beam is a superposed standing wave consisting of two standing-wave components, one being translation dominated and the other being rotation dominated. These two components correspond to two types of waves when the beam becomes infinite, termed the k_a- and k_b-waves, respectively. It should be noted that while the k_a-wave is propagating in the whole spectrum, the k_b-wave is evanescent at low frequencies and becomes propagating at frequencies higher than a critical frequency. For certain types of boundary conditions, however, a vibration mode could be made up of only one standing-wave component, either the k_a- or the k_b-component [5].

Mead [6] analyzed power flow in an infinite beam using Timoshenko beam theory, where the k_a- and k_b-waves were termed the low-speed and the high-speed waves, respectively. For the k_a-waves, the power flows due to bending and shear are equal at low frequencies while the power flow due to shear becomes larger than that due to bending at high frequencies. Only the k_b-waves at high frequencies (at which they are propagating) were considered, and the power flow due to bending is larger than that due to shear. This suggested that the k_a- and k_b-waves play different roles in transmitting energy.

Another situation in which individual roles of the k_a- and k_b-waves are of interest is beam structures with cracks. When a crack is present in a beam, it would develop under the action of local stresses when the beam is vibrating due to impulse or cyclic loading. The growth of cracks could lead to ultimate failure of the structure. Bending stress and shear stress play different roles in the growth of cracks; the former usually induces Mode I of crack propagation, i.e., the crack develops perpendicular to the direction of the crack, while the latter leads to Mode II of crack propagation, i.e., the crack develops parallel to the direction of the crack [7]. Since bending and shear are dominant in k_b- and k_a-waves at higher frequencies, respectively, a study of individual contributions of these two-wave components to bending and shear stresses will be instructive.

In the present study, the contributions of these two standing-wave components (k_a and k_b) to dynamic stresses in a beam are investigated. A uniform cantilever beam subjected to an impulse loading at the tip is taken as an example. Since Bobrovnitskii [8] showed that evanescent waves could transmit energy in a finite-length beam, the contribution of k_b-components at frequencies below the critical frequency is also considered, and particular attention is given to the variation of the contribution of the k_b-component when it changes from evanescent to propagating. The effect of force duration is also studied.

2. Theoretical analysis

2.1. Equation of motion

According to Timoshenko beam theory, the equation of motion of a uniform beam subjected to external loadings is expressed as

$$\rho A\frac{\partial^2 w(z,t)}{\partial t^2}-KGA\left(\frac{\partial^2 w(z,t)}{\partial z^2}-\frac{\partial \phi(z,t)}{\partial z}\right)=F_e(z,t),$$
$$EI\frac{\partial^2 \phi(z,t)}{\partial z^2}+KGA\left(\frac{\partial w(z,t)}{\partial z}-\phi(z,t)\right)-\rho I\frac{\partial^2 \phi(z,t)}{\partial t^2}=M_e(z,t), \quad (1)$$

where ρ is the density, A and I are the cross-sectional area and the second moment of area, respectively; E is Young's modulus, G is the shear modulus, and K is the shear coefficient. F_e and M_e are the external force and

moment, respectively. The critical frequency is given by

$$\omega_c = \sqrt{\frac{KGA}{\rho I}}. \tag{2}$$

Along with the equation of motion, the boundary conditions of the beam must be specified and they are important to the nature of vibration modes. Vibration modes of a beam with elastic end supports are superposed standing waves in general [4]. Under certain boundary conditions, e.g., simply-supported, vibration modes of a beam are not superposed standing waves but consist of one type of wave only, either k_a- or k_b-wave [5]. In the present study, the general situation of superposed standing waves is considered.

2.2. Normal modes and orthogonal relations

The normal modes are obtained by solving the governing equation, Eq. (1), when external force and moment are absent, along with corresponding boundary conditions. The general expression of superposed normal modes associated with natural frequency ω_m can be written as

$$\mathbf{S}_m(z) = \begin{Bmatrix} W_m(z) \\ \Phi_m(z) \end{Bmatrix} = \begin{Bmatrix} [A_m \sin(k_{am}z + \phi_{am})] + [B_m \sinh(k_{bm}z + \phi_{bm})] \\ q_{am}[A_m \cos(k_{am}z + \phi_{am})] + q_{bm}[B_m \cosh(k_{bm}z + \phi_{bm})] \end{Bmatrix}, \quad \text{for } \omega_m < \omega_c, \tag{3a}$$

$$\mathbf{S}_m(z) = \begin{Bmatrix} W_m(z) \\ \Phi_m(z) \end{Bmatrix} = \begin{Bmatrix} [A_m \sin(k_{am}z + \phi_{am})] + [B_m \sin(k_{bm}z + \phi_{bm})] \\ q_{am}[A_m \cos(k_{am}z + \phi_{am})] + q_{bm}[B_m \cos(k_{bm}z + \phi_{bm})] \end{Bmatrix}, \quad \text{for } \omega_m > \omega_c, \tag{3b}$$

where $m = 1, 2, 3, \ldots, k_{am}$ and k_{bm} are the wave numbers of the k_a- and k_b-wave components, respectively, $q_{am} = k_{am} - \omega_m^2/k_{am}\omega_c^2 r_g^2$, $q_{bm} = k_{bm} - \omega_m^2/k_{bm}\omega_c^2 r_g^2$, and $r_g = \sqrt{I/A}$ is the radius of gyration. In Eqs. (3), A_m, B_m, ϕ_{am}, and ϕ_{bm}, $m = 1, 2, 3, \ldots$, are constant coefficients to be determined.

The orthogonal relations of superposed normal modes have been given by Meirovitch [9], which can be written as

$$\int_0^L \mathbf{S}_m^{\mathrm{T}}(z)\hat{\mathbf{M}}\,\mathbf{S}_n(z)\,\mathrm{d}z = \delta_{mn}, \tag{4}$$

$$\int_0^L \mathbf{S}_m^{\mathrm{T}}(z)\hat{\mathbf{L}}\,\mathbf{S}_n(z)\,\mathrm{d}z = \omega_m^2\delta_{mn}, \tag{5}$$

where $\mathbf{S}_m(z)$ and $\mathbf{S}_n(z)$ are the mth and the nth normal modes, respectively. The operators are given by

$$\hat{\mathbf{M}} = \begin{pmatrix} 0 & \rho I \\ \rho A & 0 \end{pmatrix}, \tag{6}$$

$$\hat{\mathbf{L}} = \begin{pmatrix} -KGA\dfrac{\mathrm{d}}{\mathrm{d}z} & KGA - EI\dfrac{\mathrm{d}^2}{\mathrm{d}z^2} \\ -KGA\dfrac{\mathrm{d}^2}{\mathrm{d}z^2} & KGA\dfrac{\mathrm{d}}{\mathrm{d}z} \end{pmatrix}. \tag{7}$$

Using the orthogonal condition and boundary conditions, the constant coefficients A_m, B_m, ϕ_{am}, and ϕ_{bm}, $m = 1, 2, 3, \ldots$, can be determined numerically to obtain the normal superposed modes.

2.3. Forced response and dynamic stresses

2.3.1. Forced response

The steady-state response of a beam subjected to external excitations can be obtained by using the modal expansion theorem [10]. Usually, the steady-state response is written as

$$\mathbf{s}(z,t) = \sum_{m=1}^{M} \mathbf{S}_m(z)\eta_m(t) = \sum_{m=1}^{M} \begin{Bmatrix} W_m(z) \\ \Phi_m(z) \end{Bmatrix} \eta_m(t), \tag{8}$$

where $\mathbf{S}_m(z)$ is the mth normal mode, $\eta_m(t)$ is the mth generalized coordinate determined by external excitations, and M is the number of normal modes used in finding the response. In the present study, a rectangular impulse loading is considered and is given by

$$\mathbf{F}(z,t) = \begin{Bmatrix} F_e(z) \\ M_e(z) \end{Bmatrix} [u(t) - u(t-T_0)], \tag{9}$$

where $u(t)$ is the step function defined as

$$u(t) = \begin{cases} 1, & t \geqslant 0, \\ 0, & t < 0, \end{cases}$$

and T_0 is the duration of the loading.

The generalized coordinate $\eta_m(t)$ is obtained by substituting the general solution Eq. (8) into the governing equation Eq. (1), and solving the equation thus obtained. For the rectangular impulse loading, the generalized coordinate is expressed as

$$\eta_m(t) = \frac{F_{em}}{\omega_m^2} \{(1 - \cos\ \omega_m t)u(t) - [1 - \cos\ \omega_m(t-T_0)]u(t-T_0)\}, \tag{10}$$

where

$$F_{em} = \int_0^L [F_e(z)W_m(z) + M_e(z)\Phi_m(z)]\,\mathrm{d}z. \tag{11}$$

2.3.2. Dynamic stresses

Dynamic normal and shear stresses can be obtained from the transverse displacement and the bending rotation. In the vector form, they are expressed as

$$\boldsymbol{\sigma}(z,t) = \begin{Bmatrix} \sigma_{zz}(z,t) \\ \tau_{yz}(z,t) \end{Bmatrix} = \begin{Bmatrix} Ey\dfrac{\partial\phi(z,t)}{\partial z} \\ KG\left[\dfrac{\partial w(z,t)}{\partial z} - \phi(z,t)\right] \end{Bmatrix}, \tag{12}$$

where $\sigma_{zz}(z,t)$ and $\tau_{yz}(z,t)$ are normal and shear stresses, respectively. The focus of the present study is on individual contributions of the k_a- and k_b-components presented in the form of superposed modes. They are given by

$$\boldsymbol{\sigma}(z,t) = \boldsymbol{\sigma}_a(z,t) + \boldsymbol{\sigma}_b(z,t) = \begin{Bmatrix} Ey\dfrac{\partial\phi_a(z,t)}{\partial z} \\ KG\gamma_a(z,t) \end{Bmatrix} + \begin{Bmatrix} Ey\dfrac{\partial\phi_b(z,t)}{\partial z} \\ KG\gamma_b(z,t) \end{Bmatrix}, \tag{13}$$

where

$$\gamma(z,t) = \frac{\partial w(z,t)}{\partial z} - \phi(z,t)$$

is the shear angle, and the subscripts a and b represent the k_a- and the k_b-components, respectively.

3. Numerical example and discussion

An example is given to demonstrate the contributions of the two components to dynamic stresses in a beam. The example is a cantilever beam subjected to a point force at its tip as shown in Fig. 1. While the duration of the force is represented by a rectangular step function in time given by Eq. (9), its spatial part is

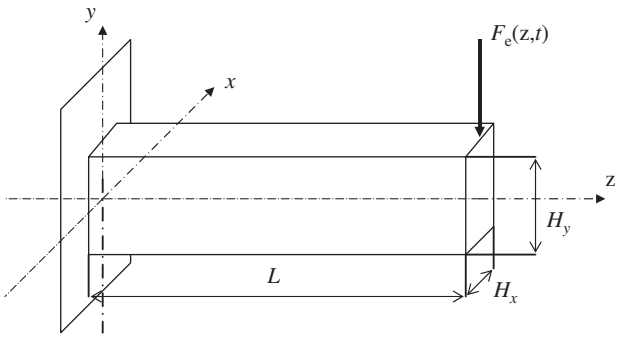

Fig. 1. A cantilever beam subjected to an impulse force at the tip.

Table 1
List of the first 20 natural frequencies of the cantilever beam

Mode number	Natural frequency (Hz)
1	83
2	496
3	1306
4	2376
5	3625
6	4993
7	6437
8	7931
9	9455
10	10 995
11	12 539
12	14 073
13	15 568
14	16 722
15	17 091
16	17 543
17	18 436
18	18 853
19	19 900
20	20 413

The critical frequency of the beam is 16 620 Hz.

expressed as

$$\mathbf{F}_e(z) = \begin{Bmatrix} F_e(z) \\ M_e(z) \end{Bmatrix} = \begin{Bmatrix} F_0\delta(z-L) \\ 0 \end{Bmatrix}, \tag{14}$$

where F_0 is the amplitude of the force, taken to be 1 N in the present example.

The beam used in this example is of rectangular cross-section, with length $L = 1$ m, the dimensions of the cross-section are $H_y = 0.1$ m and $H_x = 0.05$ m as shown in Fig. 1. The material of the beam is carbon steel with Young's modulus $E = 208 \times 10^9$ Pa, shear modulus $G = 82 \times 10^9$ Pa, and the density is $\rho = 7850\,\text{kg/m}^3$. The shear coefficient obtained by using Stephen's formula [11] is given by $K = 5(1+\nu)/(6+5\nu) = 0.864$. The critical frequency is found to be $f_c = \omega_c/2\pi = 16\,561$ Hz.

Normal mode analysis of the cantilever beam is carried out first. In Table 1 are listed the natural frequencies of the first 20 modes. There are 13 modes below the critical frequency. In the present computation, the first 20 normal modes are used to find the response, i.e., $N = 20$. For the rectangular impulse loading, the steady-state

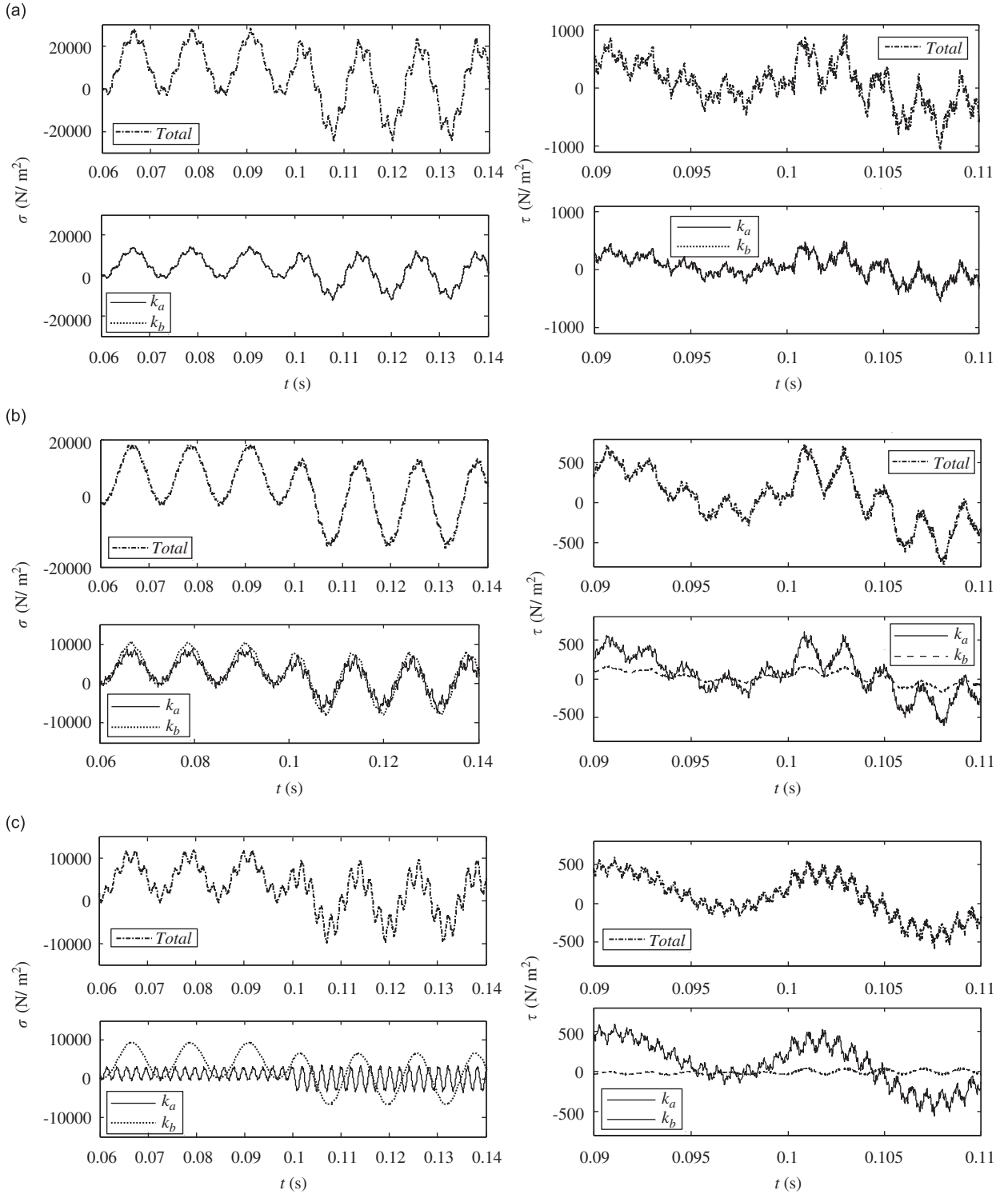

Fig. 2. Time evolutions of dynamic stresses of the cantilever beam subjected to an impulse tip force of long duration, at different locations along the span: (a) $z/L = 0$ (root); (b) $z/L = 0.25$; (c) $z/L = 0.5$; (d) $z/L = 0.75$; and (e) $z/L = 1$ (tip).

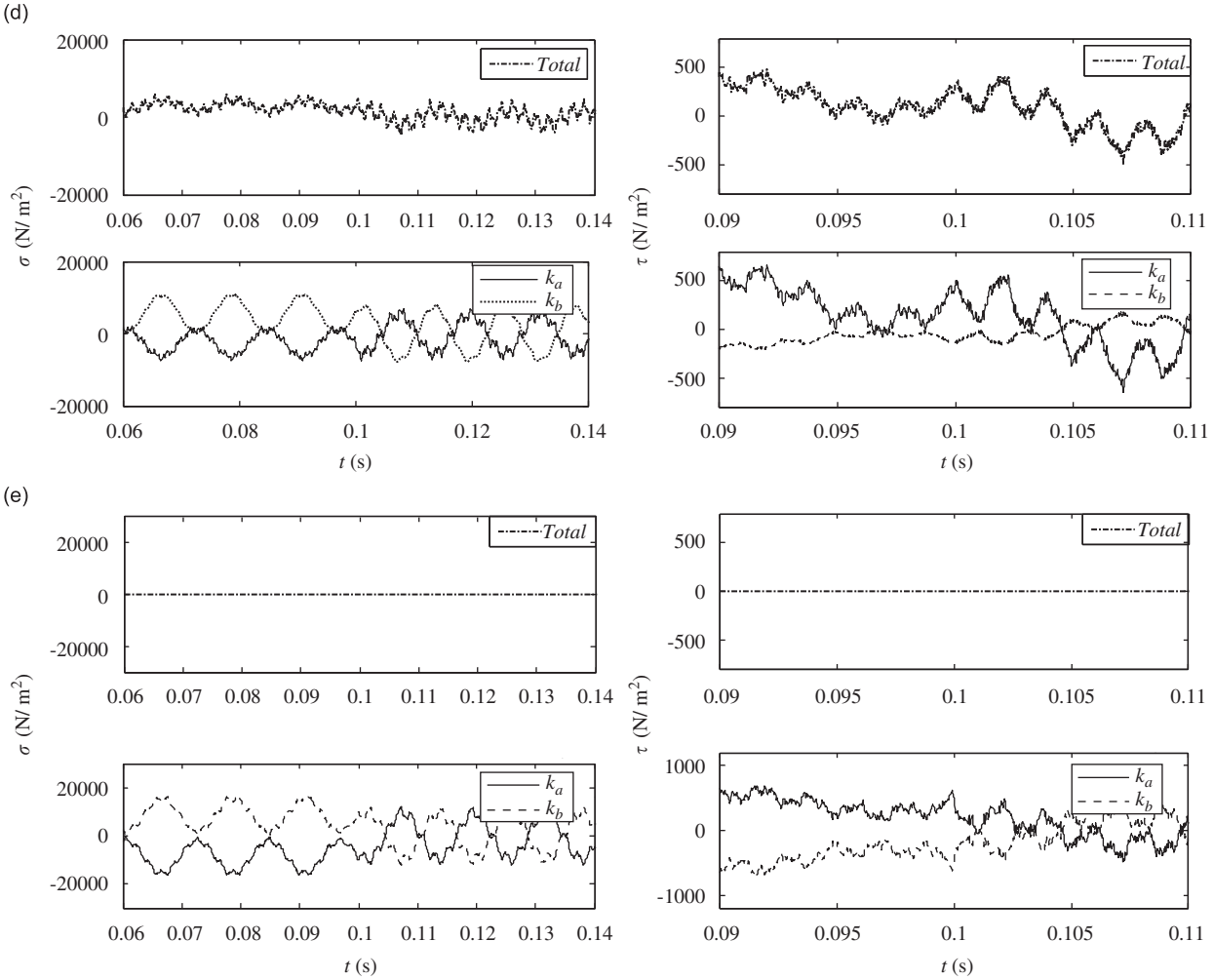

Fig. 2. (*Continued*)

response is written as

$$\mathbf{s}(z,t)=\sum_{n=1}^{N}\frac{F_0 W_n(L)}{\omega_n^2}\begin{Bmatrix} W_n(z) \\ \Phi_n(z)\end{Bmatrix}\{(1-\cos\,\omega_n t)u(t)-[1-\cos\,\omega_n(t-T_0)]u(t-T_0)\}. \tag{15}$$

Dynamic stresses can then be calculated using Eqs. (12) and (13). While the shear stress is an "averaged" one, the normal stress varies linearly over the cross-section. In the present example, the normal stress at the edge of the cross-section, i.e., its maximum value is calculated. In the following, τ and σ are used to represent the "averaged" shear stress and the maximum positive (tensile) normal stress, respectively. Two force durations, $T_0 = 0.1$ s and 10 μs, are considered in the present example. The former one is a long duration, much longer than the period of the lowest (the 1st) mode while the latter one is a short duration, shorter than the period of the highest (the 20th) mode.

3.1. Dynamic normal and shear stresses for the long-duration force

The calculated normal and shear stresses at five locations along the span, i.e., $z/L = 0$ (root), 0.25, 0.5, 0.75, and 1 (tip) are plotted in Fig. 2. Apart from total dynamic stresses, individual contributions of the two

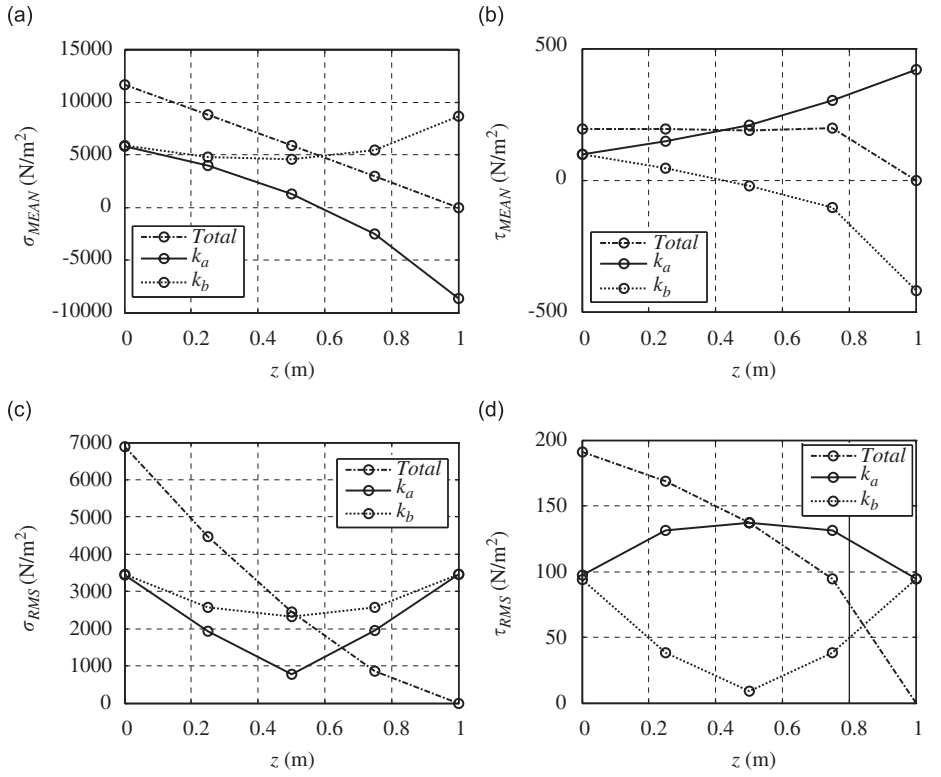

Fig. 3. Spanwise statistics of dynamic stresses of the cantilever beam subjected to an impulse tip force of long duration: the period when the force is present, $0 \leqslant t < T_0$: (a) mean normal stress; (b) rms value of normal stress; (c) mean shear stress; and (d) rms value of shear stress.

components are also plotted to demonstrate their roles. In the figures, only a portion of each set of data is plotted so that a qualitative but clear picture can be illustrated. For quantitative assessment, the corresponding mean and root-mean-square (rms) values of the stresses are calculated and plotted in Figs. 3 and 4 for the periods when the force is present ($0 \leqslant t < T_0$) and absent ($t \geqslant T_0$), respectively. The mean values of the stresses give the static stresses, whereas the rms values of the stresses represent the magnitudes of dynamic stresses. The phase difference between the two components are also calculated and plotted in Fig. 5.

For either normal or shear stress, the contributions of the two components appear to be equal and in-phase at the root while equal and out-of-phase at the tip of the cantilever beam, as seen from Fig. 2. While the out-of-phase relation at the tip is expected since they have to be superposed to give rise to zero normal and shear stresses, the in-phase relation at the root cannot be understood readily. To facilitate easy interpretation of the results, a theoretical analysis is given in Section 3.3. Along the beam span from root to tip, the k_b-component of the normal stress becomes larger while the k_a-component of the shear stress becomes larger. Further quantitative comparison of their individual contributions is illustrated by their mean and rms values, as shown in Figs. 3 and 4.

In Fig. 3 are plotted the mean and rms values of the stresses when the force is applied ($0 \leqslant t < T_0$). During this period, the beam experiences both static and dynamic stresses. For the static normal and shear stresses shown in Figs. 3a and b, respectively, the two components show different trends in their spanwise variation. For the normal stress, the k_a-component decreases linearly from positive to negative as seen in Fig. 3a; thus implying that it undergoes a transition from tensile to compressive. However, the k_b-component is always positive (tensile) and remains constant essentially, except near the tip where it is increased to balance the k_a-component at the tip. Therefore, the linear variation of total normal stress is due to the k_a-component. However, the total normal stress is kept positive (tensile) since the magnitude of the k_b-component is larger than that of the k_a-component. In this sense, the k_b-component dominates in the static normal stress. If a crack is present in the beam and develops in Mode I, then the k_b-component would play a dominant role.

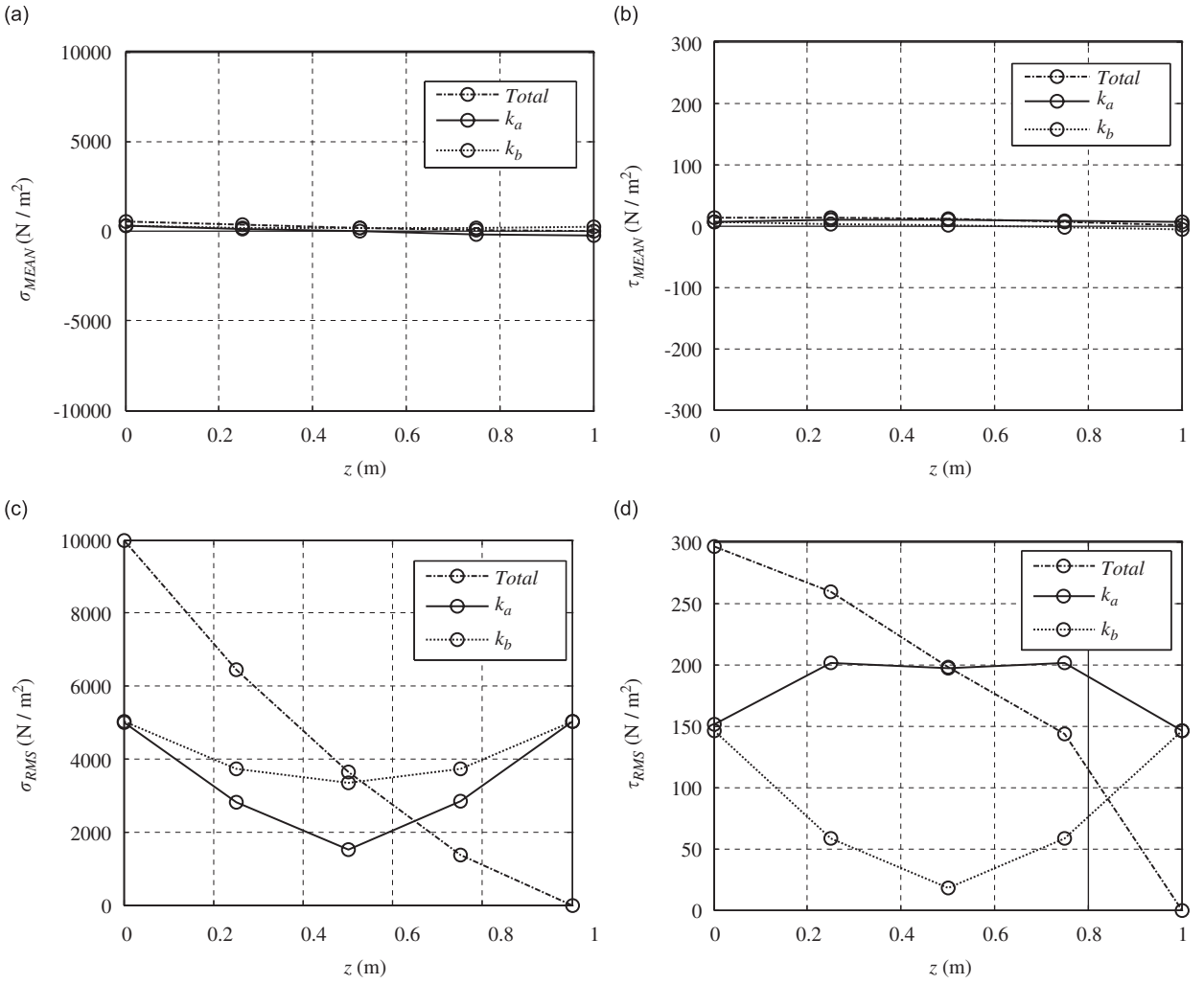

Fig. 4. Spanwise statistics of dynamic stresses of the cantilever beam subjected to an impulse tip force of long duration: the period when the force is absent, $t \geqslant T_0$: (a) mean normal stress; (b) rms value of normal stress; (c) mean shear stress; and (d) rms value of shear stress.

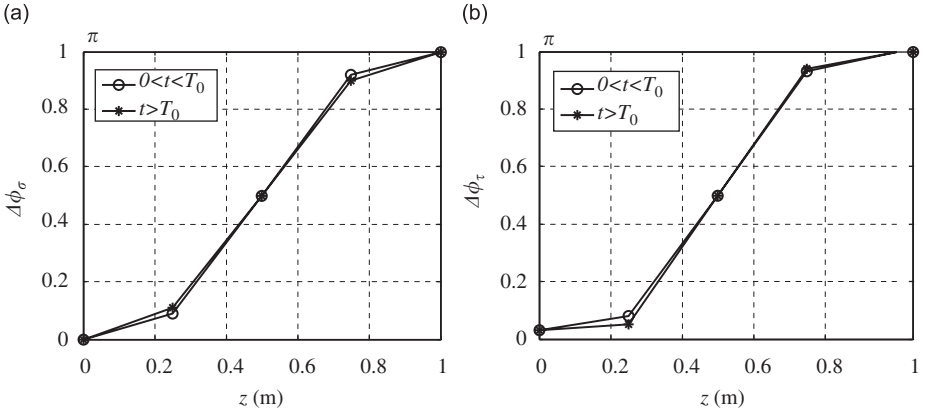

Fig. 5. Phase differences between the k_a- and the k_b-components of dynamic stresses in the cantilever beam subjected to an impulse tip force of long duration: (a) phase difference between normal stresses, $\Delta\phi_\sigma$; and (b) phase difference between shear stresses, $\Delta\phi_\tau$.

For the static shear stress, the k_b-component decreases linearly from positive to negative as seen in Fig. 3b, except near the tip where it suddenly drops to balance the k_a-component at the tip. The k_a-component increases almost linearly and remains positive, and its magnitude is larger than that of the k_b-component. As a result, the total shear stress is constant and positive along the beam span, except near the tip. Therefore, the k_a-component would play a dominant role if a crack in the beam develops in Mode II.

Different from static stresses, the rms values of the total dynamic normal and shear stresses show quadratic variation along the span, as shown in Figs. 3c and d, respectively. For the normal stress, both the k_a- and the k_b-components first decrease and then increase along the beam span from root to tip, as seen in Fig. 3c. Their minimum values occur at the mid-span. The rms value of the k_b-component is larger than that of the k_a-component, implying that it dominates the dynamic normal stress. However, the spanwise variation of the normal stress does not follow that of the k_b-component, but shows a quadratic decrease. This can be attributed to the phase difference between the two components as shown in Fig. 5a. The phase difference is close to zero (in-phase) near the root and close to π (out-of-phase) near the tip. In between, the phase difference shows a linear variation, and is equal to $\pi/2$ at mid-span. The rms value of the total normal stress is approximately equal to the k_b-component, thus it is the dominant one. If a crack at mid-span develops in Mode I, the k_b-component will play a dominant role in the growth of the crack.

For the shear stress, the k_a-component first increases then decreases, with a maximum value at mid-span while the k_b-component first decreases then increases, with a minimum value at mid-span, as seen in Fig. 4d. As a result, the total shear stress shows a quadratic decrease but its feature of variation is different from that of the normal stress. This increases the possibility for a crack at the mid-span to develop in Mode II. The spanwise variation of phase difference is similar to that for the normal stress, as seen in Fig. 5b. For the dynamic shear stress, the k_a-component is dominant. Therefore, it should play a significant role if a crack develops in Mode II.

After the impulse force is removed ($t > T_0$), the static stresses become approximately zero as shown in Figs. 4a and b. The behavior of the spanwise variation of the dynamic stresses remains the same as shown in Figs. 4c and d, so does that of the phase relationship as shown in Fig. 5b. However, the rms values of the dynamic stresses are increased. This enhances the possibility of crack growth in both modes of crack propagation.

One noteworthy feature of the k_b-component is that its wave character transits from evanescent to propagating when its frequency exceeds a critical value, ω_c. The influence of this transition on the contribution of the k_b-component to the stresses is studied by calculating the ratios of the rms values of the k_b- and the k_a-components, in the frequency range below and above ω_c, respectively. The ratios below and above ω_c indicate the contributions of the evanescent and the propagating k_b-component, respectively. The results calculated at mid-span of the beam are given in Table 2. It can be seen that the contribution of the evanescent k_b-components is significant in the normal stress but very small in the shear stress. This suggests that evanescent k_b-components play an important role in the normal stress. Furthermore, since the ratios are calculated using the data at the mid-span of the beam, the result also suggests that the influence of evanescent waves might not be limited to the near field as usually assumed.

Table 2
Comparison of the relative contributions of evanescent and propagating k_b-components at mid-span of the cantilever beam subjected to an impulse tip force of long duration

	Evanescent k_b-components ($\omega < \omega_c$)	Propagating k_b-components ($\omega > \omega_c$)
(a) $0 \leqslant t < T_0$		
$\sigma_{\mathrm{rms},b}/\sigma_{\mathrm{rms},a}$	2.98	0.98
$\tau_{\mathrm{rms},b}/\tau_{\mathrm{rms},a}$	0.06	1.15
(b) $t > T_0$		
$\sigma_{\mathrm{rms},b}/\sigma_{\mathrm{rms},a}$	2.21	0.94
$\tau_{\mathrm{rms},b}/\tau_{\mathrm{rms},a}$	0.09	1.24

3.2. Dynamic normal and shear stresses for the short-duration force

The influence of short duration of force is also considered in the present study. Since the time duration is very short in this case ($T_0 = 10\,\mu s$), the focus is on the dynamic stresses during the period $t > T_0$. The calculated dynamic stresses at five locations along the span, i.e., $z/L = 0$ (root), 0.25, 0.5, 0.75, and 1 (tip), are plotted in Fig. 6. Corresponding mean and rms values along the span are calculated and the results are plotted in Fig. 7. The mean values are approximately zeroes as shown in Figs. 7a and b. This is expected since the static stresses diminish after the force is removed. The phase difference between the k_a- and the k_b-components are plotted in Fig. 8.

As seen from Fig. 6e, the behavior at the tip is similar to the case of long-duration force. The two components are out-of-phase, and their contributions to the total dynamic stresses are equal. This is confirmed by the statistics shown in Fig. 7 and the phase relationship shown in Fig. 8. At the root, the two components appear to be in-phase, but as seen from Fig. 8, they have a slight phase difference in reality. For the normal stress, the k_b-component is slightly larger; while for the shear stress, the k_a-component is larger, as shown in Fig. 7. From the root to the tip, the contribution of the k_a-component appears to be larger for both the normal and the shear stresses.

In Figs. 7c and d are plotted the rms values of dynamic normal and shear stresses along the beam span. It can be seen that the rms values of the total stresses decrease from their maximum values at the root, become uniform along the span, and then decrease further to zero at the tip. This is rather different from the case of a long-duration force, in which a quadratic decrease is observed. Moreover, the magnitudes of the dynamic normal and shear stresses are much lower than those in the case of a long-duration force. This suggests that the possibility for a crack to develop in either mode of propagation is significantly reduced.

Individual contributions of the two components also show some different features. They appear to be uniform along the span in the middle section of the beam covering $z/L = 0.2$–0.8. In this section, the k_a-components are dominant in both normal and shear stresses. This implies that, once a crack grows under the action of a short-duration force, the k_a-component plays a dominant role in spite of the modes of crack propagation. The variation of the phase difference between the two components can be seen from Fig. 8. For either normal or shear stress, the phase difference in the mid-span of the beam appears to be uniform and its value is $\pi/2$.

The contribution of the k_b-component when it transits from evanescent to propagating is also investigated. In Table 3 are given the ratios of the rms value of the k_b-component to that of the k_a-component at the mid-span of the beam, in the frequency range below and above the critical frequency, respectively. It can be seen that the contribution of evanescent k_b-components to the normal stress becomes less significant for the case of short-duration excitation.

3.3. Further analysis of the phase relationship between the k_a and k_b components

From the above analysis, it is seen that the phase relationship between the two components affects their individual contributions. At the root (clamped end) and the tip (free end), the two components have equal contributions, but in-phase and out-of-phase, respectively. While the out-of-phase relationship at the tip is expected, an analysis of the phase relationship at the root and along the beam span would be instructive. Only the normal and the shear stresses in the period $t \geqslant T_0$ are analyzed in the following, since the behavior of phase difference is similar in the period $0 \leqslant t < T_0$.

Consider the normal stress first. Using Eqs. (13) and (15), the expression of the maximum tensile normal stress can be written as

$$\sigma(z,t) = \sigma_a(z,t) + \sigma_b(z,t), \tag{16a}$$

where

$$\sigma_a(z,t) = \frac{EH_y}{2} \sum_{n=1}^{20} \frac{F_0 W_n(L)}{\omega_n^2} \Phi'_{an}(z) \cos(\omega_n t + \theta_{tn}), \tag{16b}$$

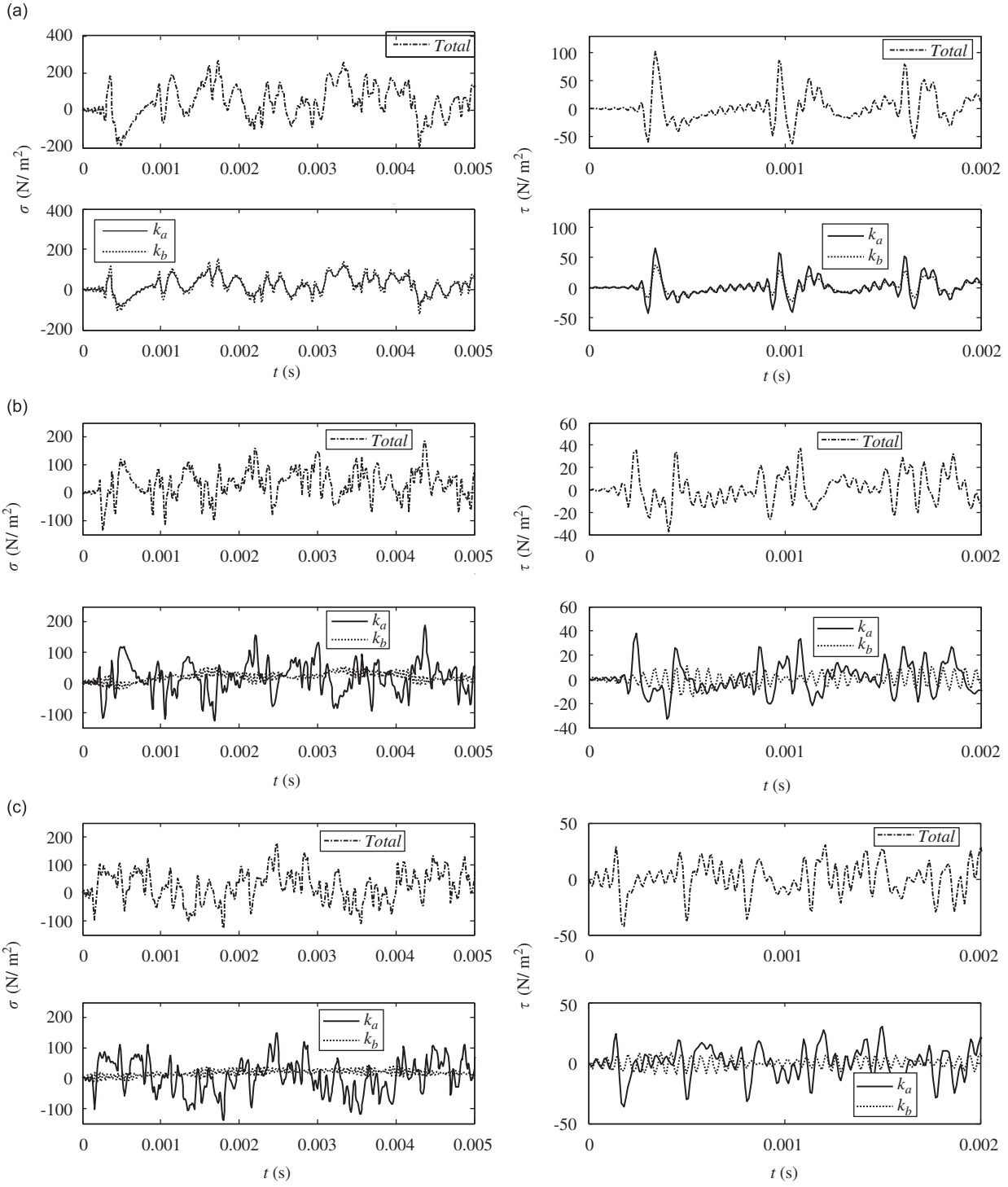

Fig. 6. Time evolutions of dynamic stresses of the cantilever beam subjected to an impulse tip force of short duration at different locations along the span: (a) $z/L = 0$ (root); (b) $z/L = 0.25$; (c) $z/L = 0.5$; (d) $z/L = 0.75$; and (e) $z/L = 1$ (tip).

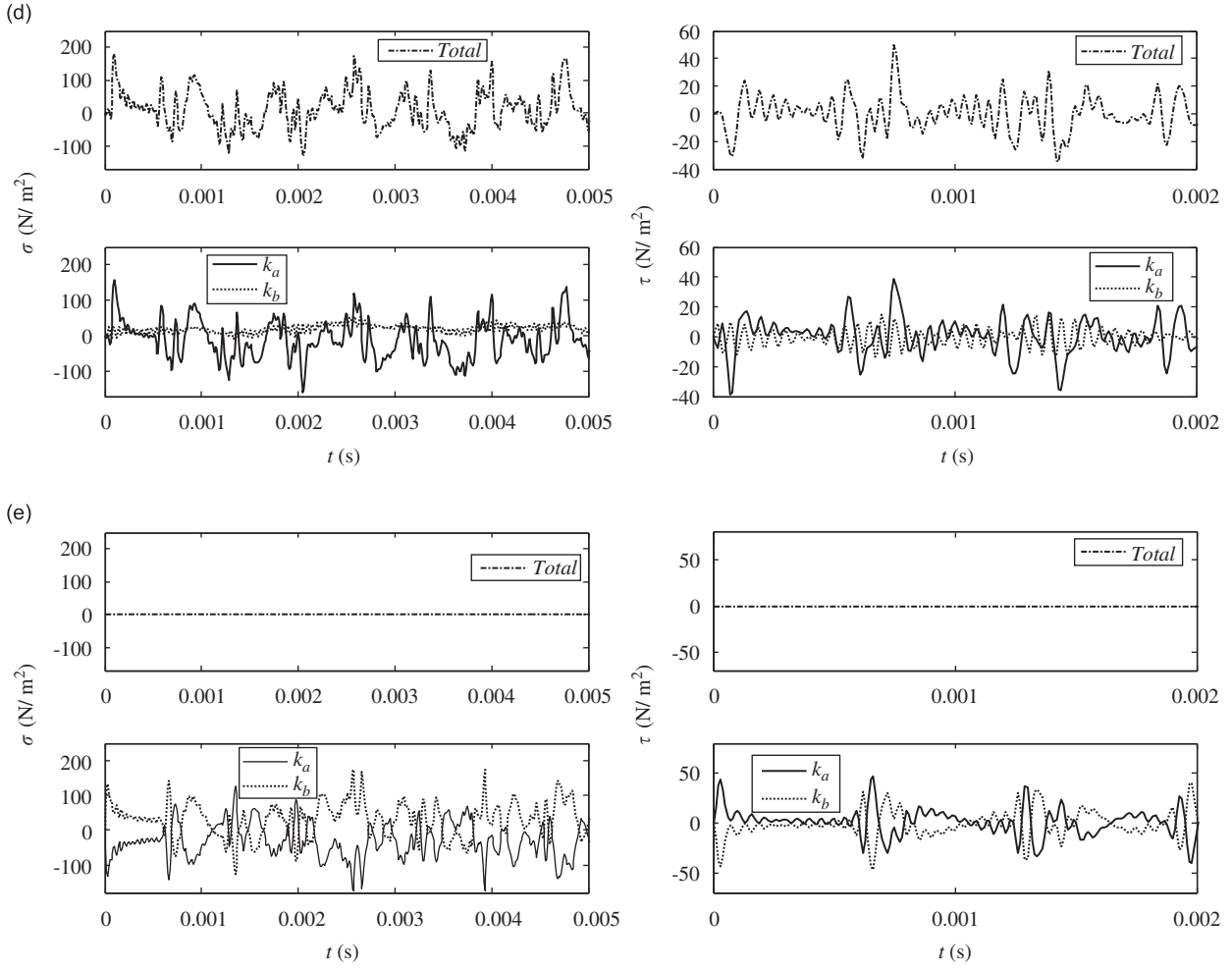

Fig. 6. (*Continued*)

$$\sigma_b(z,t) = \frac{EH_y}{2}\sum_{n=1}^{20}\frac{F_0 W_n(L)}{\omega_n^2}\Phi'_{bn}(z)\cos(\omega_n t + \theta_{tn}), \tag{16c}$$

$$\theta_{tn} = \tan^{-1}\left(\frac{\sin\,\omega_n T_0}{1-\cos\,\omega_n T_0}\right). \tag{16d}$$

It can be seen that the phase relationship between the k_a- and k_b-components of the normal stress is determined by the relationships between $\Phi'_{an}(z)$ and $\Phi'_{bn}(z)$, which are expressed as

$$\Phi'_{an}(z) = -q_{an}k_{an}A_n\sin(k_{an}z+\phi_{an}), \quad n=1,2,\ldots,20, \tag{17a}$$

$$\Phi'_{bn}(z) = \begin{cases} q_{bn}k_{bn}B_n\sinh(k_{bn}z+\phi_{bn}), & n=1,2,\ldots,13,\\ -q_{bn}k_{bn}B_n\sin(k_{bn}z+\phi_{bn}), & n=14,15,\ldots,20. \end{cases} \tag{17b}$$

Each mode has to satisfy the boundary conditions individually. At the root (clamped end), the boundary conditions for each mode can be written as

$$\begin{aligned} &A_n\sin\,\phi_{an} + B_n\sinh\,\phi_{bn} = 0,\\ &q_{an}A_n\cos\,\phi_{an} + q_{bn}B_n\cosh\,\phi_{bn} = 0, \quad n=1,2,\ldots,13, \end{aligned} \tag{18a}$$

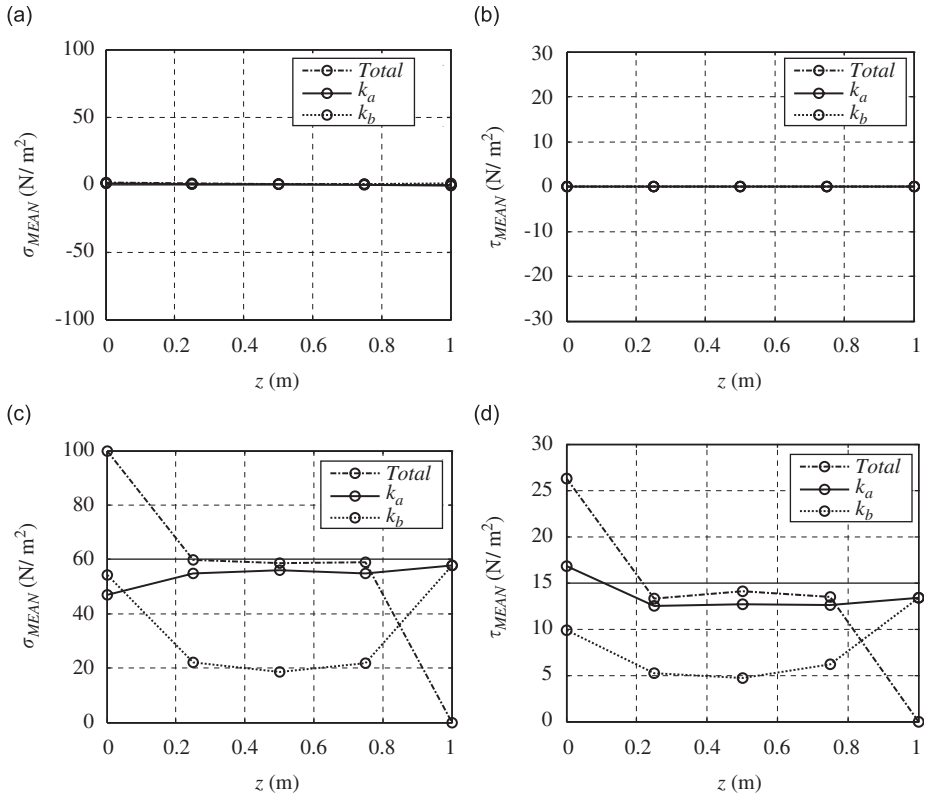

Fig. 7. Spanwise statistics of dynamic stresses of the cantilever beam subjected to an impulse tip force of short duration: (a) mean normal stress; (b) rms value of normal stress; (c) mean shear stress; and (d) rms value of shear stress.

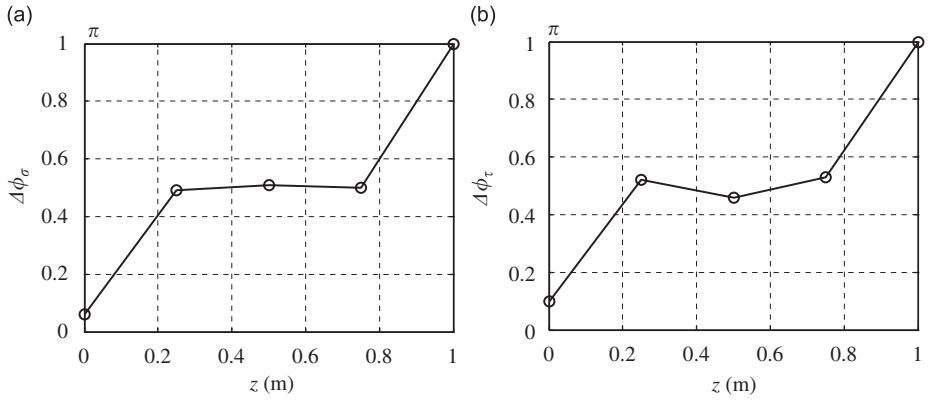

Fig. 8. Phase differences between the k_a-and the k_b-components of dynamic stresses in the cantilever beam subjected to an impulse tip force of short duration: (a) phase difference between normal stresses, $\Delta\phi_\sigma$; and (b) phase difference between shear stresses, $\Delta\phi_\tau$.

$$A_n \sin \phi_{an} + B_n \sin \phi_{bn} = 0,$$
$$q_{an} A_n \cos \phi_{an} + q_{bn} B_n \cos \phi_{bn} = 0, \quad n = 14, 15, \ldots, 20. \tag{18b}$$

From Eqs. (18a) and (18b), the following relations can be obtained,

$$A_n \sin \phi_{an} = -B_n \sinh \phi_{bn}, \quad n = 1, 2, \ldots, 13, \tag{19a}$$

Table 3
Comparison of the relative contributions of evanescent and propagating k_b-components at mid-span of the cantilever beam subjected to an impulse tip force of short duration

	Evanescent k_b-components ($\omega<\omega_c$)	Propagating k_b-components ($\omega>\omega_c$)
$\sigma_{rms,b}/\sigma_{rms,a}$	0.31	0.98
$\tau_{rms,b}/\tau_{rms,a}$	0.03	1.15

$$A_n \sin \phi_{an} = -B_n \sin \phi_{bn}, \quad n = 14, 15, \ldots, 20. \tag{19b}$$

Furthermore, at the root,

$$\frac{\Phi'_{an}(0)}{\Phi'_{bn}(0)} = \begin{cases} -\dfrac{q_{an}k_{an}A_n \sin \phi_{an}}{q_{bn}k_{bn}B_n \sinh \phi_{bn}} = \dfrac{q_{an}k_{an}}{q_{bn}k_{bn}}, & n = 1, 2, \ldots, 13, \\ \dfrac{q_{an}k_{an}A_n \sin \phi_{an}}{q_{bn}k_{bn}B_n \sin \phi_{bn}} = -\dfrac{q_{an}k_{an}}{q_{bn}k_{bn}}, & n = 14, 15, \ldots, 20, \end{cases} \tag{20}$$

From the dispersion relations of the k_a- and k_b-waves given by Chan et al. [4], it can be deduced that $q_{an}k_{an}>0$ for $n = 1, 2, \ldots, 20$, while $q_{bn}k_{bn}>0$ for $n = 1, 2, \ldots, 13$ and $q_{bn}k_{bn}<0$ for $n = 14, 15, \ldots, 20$. From Eq. (20), it can be deduced that $\Phi'_{an}(0)$ and $\Phi'_{bn}(0)$ are of the same sign for each mode. Therefore, for the normal stress at the root, the k_a- and k_b-components of each mode are thus in-phase, and their summations are expected to be in-phase.

Secondly, consider the shear stress. Using Eqs. (13) and (15), they are expressed as

$$\tau(z, t) = \tau_a(z, t) + \tau_b(z, t), \tag{21a}$$

where

$$\tau_a(z, t) = KG \sum_{n=1}^{20} \frac{F_0 W_n(L)}{\omega_n^2} H_{an}(z) \cos(\omega_n t + \theta_{tn}), \tag{21b}$$

$$\tau_b(z, t) = KG \sum_{n=1}^{20} \frac{F_0 W_n(L)}{\omega_n^2} H_{bn}(z) \cos(\omega_n t + \theta_{tn}), \tag{21c}$$

$$H_n(z) = \frac{\mathrm{d}W_n(z)}{\mathrm{d}z} - \Phi_n(z) \quad \text{and} \quad \theta_{tn} = \tan^{-1}\left(\frac{\sin \omega_n T_0}{1 - \cos \omega_n T_0}\right). \tag{21d}$$

It can be seen that the phase relationship between the k_a- and k_b-components of the shear stress is determined by the relationships between $H_{an}(z)$ and $H_{bn}(z)$, which are expressed as

$$H_{an}(z) = (k_{an} - q_{an})A_n \cos(k_{an}z + \phi_{an}), \tag{22a}$$

$$H_{bn}(z) = \begin{cases} (k_{bn} - q_{bn})B_n \cosh(k_{bn}z + \phi_{bn}), & n = 1, 2, \ldots, 13, \\ (k_{bn} - q_{bn})B_n \cos(k_{bn}z + \phi_{bn}), & n = 14, 15, \ldots, 20. \end{cases} \tag{22b}$$

At the root, their ratio is expressed as

$$\frac{H_{an}(0)}{H_{bn}(0)} = \begin{cases} \dfrac{(k_{an} - q_{an})A_n \cos \phi_{an}}{(k_{bn} - q_{bn})B_n \cosh \phi_{bn}}, & n = 1, 2, \ldots, 13, \\ \dfrac{(k_{an} - q_{an})A_n \cos \phi_{an}}{(k_{bn} - q_{bn})B_n \cos \phi_{bn}}, & n = 14, 15, \ldots, 20. \end{cases} \tag{23}$$

From Eqs. (18a) and (18b), another two relations can be obtained, they are

$$q_{an}A_n \cos \phi_{an} = -q_{bn}B_n \cosh \phi_{bn}, \quad n = 1, 2, \ldots, 13, \tag{24a}$$

$$q_{an}A_n \cos \phi_{an} = -q_{bn}B_n \cos \phi_{bn}, \quad n = 14, 15, \ldots, 20. \tag{24b}$$

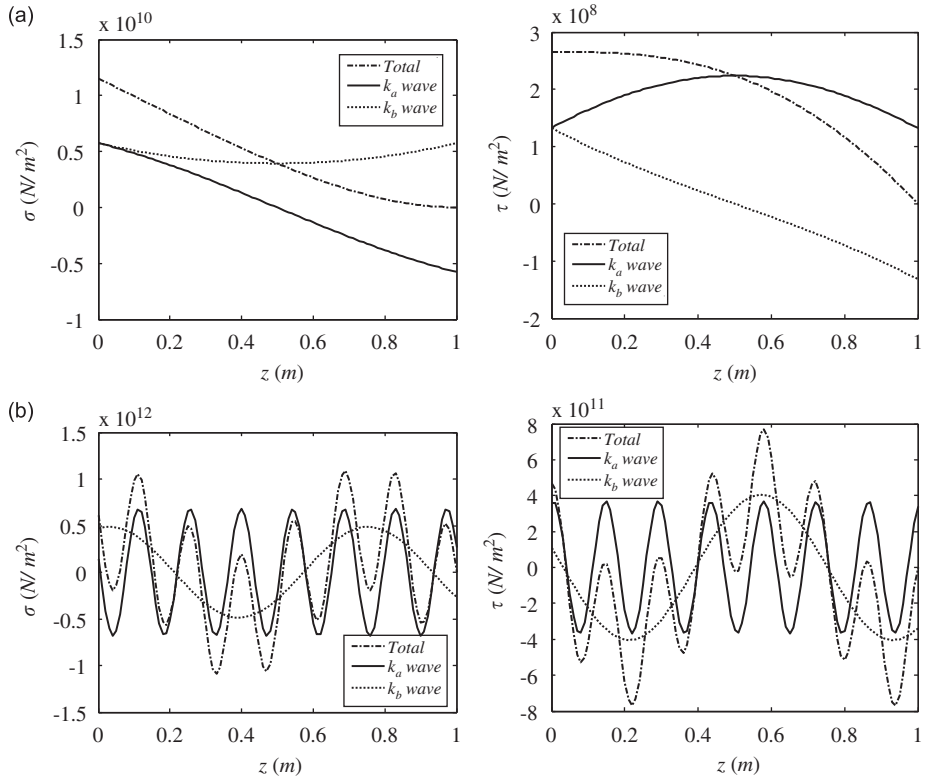

Fig. 9. Spanwise variation of dynamic stresses for two modes of the cantilever beam subjected to an impulse tip force of short duration: (a) Mode 1 and (b) Mode 17.

From the dispersion relations of the k_a- and k_b-waves given by Chan et al. [4], it can be deduced that $q_{an}/(k_{an}-q_{an})>0$, while $q_{bn}/(k_{bn}-q_{bn})<0$. From Eqs. (23), (24a) and (24b), it can be deduced that $H_{an}(z)$ and $H_{bn}(z)$ are of the same sign for each mode. Therefore, for the shear stress at the root, the k_a- and k_b-components of each mode are in-phase, and their summations are expected to be in-phase too.

The in-phase relationship at the root and the out-of-phase relationship at the tip can be termed as definite in the sense that the two components for each mode have the same phase relation, thus the overall relationships are not affected by modal summation. At a position along the beam span, however, the situation is different.

For the normal stress, the phase relation between the two components is determined by the phase difference between $\Phi'_{an}(z)$ and $\Phi'_{bn}(z)$. Referring to Eqs. (17a) and (17b), it can be seen that $\Phi'_{an}(z)$ and $\Phi'_{bn}(z)$ could be of the same or of the opposite sign, thus the k_a- and k_b-components are either in-phase or out-of-phase. This is illustrated by Fig. 9, where the k_a- and k_b-components of dynamic stresses for Modes 1 and 17 are shown. Natural frequencies of these two modes are below and above the critical frequency, respectively. It can be seen that the two components are in-phase at the root and out-of-phase at the tip for both modes. However, the phase relation between the two components varies along the span and is different for different mode. Therefore, the phase relationship is not as definite as at the ends of the beam. While the phase difference of 0 or π implies that the two components are well correlated (-1 or 1), the phase difference of $\pi/2$ means that they are uncorrelated. The phase relation between the two components (each summed over the first 20 modes) becomes about $\pi/2$, exhibiting a modal-summation-induced local degradation of correlation between the two components over the middle span length of the cantilever. The phenomenon is more marked for the case of short-duration impact because it should generate more high-frequency modes.

4. Conclusions

Individual contributions of two standing-wave components to the normal and shear dynamic stresses in a beam are studied, and their roles in crack development in a beam are briefly addressed. In particular, the contribution of the k_b-component, whose wave character transits from evanescent to propagating at a critical frequency, is investigated.

The beam considered is a cantilever subjected to an impulse loading at its tip, with two different time durations, one much shorter than the period of the 20th mode, and the other much longer than the period of the 1st mode, representing short and long duration of the force, respectively. For a long-duration impulse loading, the normal and the shear stresses are dominated by the k_b- and the k_a-components, respectively. For a short-duration impulse loading, both the normal and shear stresses are dominated by the k_a-component. The magnitudes of normal and shear stresses in the case of a long-duration force are much higher than those in the case of a short-duration force; hence the possibility of crack growth is higher. In the case of a long-duration force, the k_b- and the k_a-components play dominant roles for crack growth in Mode I and Mode II, respectively. In the case of a short-duration force, however, the k_a-component plays the dominant role for crack growth in either Mode I or Mode II.

Further analysis shows that the evanescent k_b-component plays an important role in the normal stress in the case of long-duration excitation, while becomes less important in the case of short-duration excitation. For the propagating k_b-component, in the case of both long- and short-duration forces, the contribution is almost the same as that of the k_a-components.

The boundary conditions also affect the contributions of the two components to total stresses. For the cantilever beam investigated, the two components are of the same amplitude and out-of-phase at the free end as expected. At the clamped end, they are in-phase and their amplitudes are almost equal. A theoretical analysis is given, showing that this is due to the influence of specific boundary conditions. From a boundary to the mid-span, the variation of phase difference is different for long and short force duration. For a long-duration impulse loading, the phase difference changes to $\pi/2$ at a location near the mid-span; while for a short-duration impulse loading, the phase difference changes to $\pi/2$ at a location closer to the boundaries.

Acknowledgements

Funding support given by the Research Grants Council of the Government of the HKSAR under Project Nos. PolyU5148/00E, PolyU5161/00E, and PolyU1/02C are gratefully acknowledged. The authors are also grateful to the reviewers for their constructive comments and advice.

References

[1] A.M. Ebner, D.P. Billington, Steady-state vibrations of damped Timoshenko beam, *ASCE Journal of Structural Division* 94 (1968) 756–764.
[2] P.K. Roy, N. Ganesan, Transient response of a cantilever beam subjected to an impulse load, *Journal of Sound and Vibration* 183 (1995) 873–890.
[3] K.F. Graff, *Wave Motion in Elastic Solids*, Dover Publications, New York, 1991.
[4] K.T. Chan, X.Q. Wang, R.M.C. So, S.R. Reid, Superposed standing waves in a Timoshenko beam, *Proceedings of the Royal Society of London A: Mathematical, Physical, and Engineering Sciences* 458 (2002) 83–108.
[5] X.Q. Wang, R.M.C. So, Various standing waves in a Timoshenko beam, *Journal of Sound and Vibration* 280 (2005) 311–328.
[6] D.J. Mead, Wave propagation in Timoshenko beams, *Strojnicky Casopis* 36 (1985) 556–584.
[7] H. Tada, P.C. Paris, G.R. Irwin, *The Stress Analysis of Cracks Handbook*, Del Research Corporation, Heller town, PA, 1973.
[8] Y.I. Bobrovnitskii, On the energy flow in evanescent waves, *Journal of Sound and Vibration* 152 (1992) 175–176.
[9] L. Meirovitch, *Principles and Techniques of Vibrations*, Prentice-Hall, Upper Saddle River, NJ, 1997.
[10] L. Meirovitch, *Fundamentals of Vibrations*, McGraw-Hill, New York, 2001.
[11] N.G. Stephen, Mindlin plate theory: best shear coefficient and higher spectra validity, *Journal of Sound and Vibration* 202 (1997) 539–553.